

---

This is an electronic reprint of the original article.  
This reprint may differ from the original in pagination and typographic detail.

Lehtinen, Petri O.; Foster, A. S.; Ayuela, A.; Krasheninnikov, A.; Nordlund, K.; Nieminen, R. M.

**Magnetic properties and diffusion of adatoms on a graphene sheet**

*Published in:*  
Physical Review Letters

*DOI:*  
[10.1103/PhysRevLett.91.017202](https://doi.org/10.1103/PhysRevLett.91.017202)

Published: 01/01/2003

*Document Version*  
Publisher's PDF, also known as Version of record

*Please cite the original version:*  
Lehtinen, P. O., Foster, A. S., Ayuela, A., Krasheninnikov, A., Nordlund, K., & Nieminen, R. M. (2003). Magnetic properties and diffusion of adatoms on a graphene sheet. *Physical Review Letters*, 91(1), 1-4. [017202]. <https://doi.org/10.1103/PhysRevLett.91.017202>

---

This material is protected by copyright and other intellectual property rights, and duplication or sale of all or part of any of the repository collections is not permitted, except that material may be duplicated by you for your research use or educational purposes in electronic or print form. You must obtain permission for any other use. Electronic or print copies may not be offered, whether for sale or otherwise to anyone who is not an authorised user.

## Magnetic Properties and Diffusion of Adatoms on a Graphene Sheet

P. O. Lehtinen,<sup>1</sup> A. S. Foster,<sup>1</sup> A. Ayuela,<sup>1</sup> A. Krasheninnikov,<sup>2</sup> K. Nordlund,<sup>2</sup> and R. M. Nieminen<sup>1</sup>

<sup>1</sup>Laboratory of Physics, Helsinki University of Technology, P.O. Box 1100, 02015, Finland

<sup>2</sup>Accelerator Laboratory, University of Helsinki, P.O. Box 43, FIN-00014 Helsinki, Finland

(Received 22 January 2003; published 30 June 2003)

We use *ab initio* methods to calculate the properties of adatom defects on a graphite surface. By applying a full spin-polarized description to the system we demonstrate that these defects have a magnetic moment of about  $0.5\mu_B$  and also calculate its role in diffusion over the surface. The magnetic nature of these intrinsic carbon defects suggests that it is important to understand their role in the recently observed magnetism in pure carbon systems.

DOI: 10.1103/PhysRevLett.91.017202

PACS numbers: 75.75.+a, 68.43.Bc, 75.70.Rf

As the techniques for growth and preparation of carbon nanostructures have developed, the list of feasible applications has seen rapid increases [1,2]. However, concurrent to this growth of technological possibilities has been an increase in the demand for atomic-scale understanding of the processes which determine carbon nanostructure properties. Studies of radiation effects [3] in graphite and other carbon nanostructures and experiments on as-grown nanotubes [4,5] have demonstrated that intrinsic carbon defects are a common phenomenon in standard samples. Understanding the properties of these defects has become an essential part of such diverse processes in carbon materials such as strain [6], lithium storage in nanotube based batteries [7], catalytic growth [8], junctions [9], and quantum dot creation [5,10]. Possibly even more importantly, the recent experimental demonstrations of magnetism in pure carbon systems [11–15] have ignited speculation that carbon could offer the tantalizing prospect of a zero-gap, high-temperature, ferromagnetic semiconductor. Several studies have speculated that intrinsic carbon defects could be responsible for the observed magnetic properties [11]. Experimentally the role of these defects is just being explored [16], yet theoretical analysis lags somewhat behind.

One of the most common defects to be created is the carbon vacancy-adatom pair [3], and therefore it is important to study the influence this kind of defect will have on the surface physical and electronic structure. For example, defect evolution is mainly determined by the mobility of vacancies and interstitials at the surface. Defects either disappear by recombination with defects of opposite character or cluster with defects of similar character, and the temperature dependence of these processes is determined by defect mobility. From experiments, in general the adatom is expected to be much more mobile in the bulk and at the surface [3] than the vacancy, and therefore its mobility is the rate determining factor. Hence, for example, knowledge of adatom migration properties is crucial in nanotube growth processes [8]. Some previous first principle theoretical studies have considered adsorption [8,17] and diffusion [18] of a car-

bon adatom on a graphene sheet, yet the results were markedly different, and none of them fully implemented the generalized gradient approximation (GGA), known to provide better accuracy for studying surface adsorption and diffusion [19,20]. Also, none of these studies systematically considered the influence of the spin density properties of the adsorbed adatom. In this Letter we study the adsorption energy and diffusion of carbon adatoms on a graphene sheet using first principles techniques and demonstrate that these defects are highly mobile and magnetic.

All the calculations have been performed using the plane wave basis VASP [21,22] code, implementing the spin-polarized density functional theory (DFT) and the GGA of Perdew and Wang [23] known as PW91. We have used projector augmented wave (PAW) potentials [24,25] to describe the core ( $1s^2$ ) electrons, with the  $2s^2$  and  $2p^2$  electrons of carbon considered as valence electrons. A kinetic energy cutoff of 400 eV was found to converge the total energy of our systems to within meV. All calculations were also converged to meV in total energy with respect to the  $\mathbf{k}$ -point sampling of the Brillouin zone. To determine the applicability of this method to study carbon based systems we initially studied bulk graphite and diamond using both the PAW and the more standard ultrasoft pseudopotential (UPP) methods. We found no significant difference between PAW and UPP, and both gave excellent agreement with experimentally determined structural parameters for both graphite and diamond. This gave us confidence that VASP and the PAW method are reliable and flexible enough to move to more complex carbon systems.

Initially calculations with the single graphite layer were made using a 50 atom slab, but all properties were also tested with larger 72 and 98 atom slabs. A single layer of graphite provides both a good model of the graphite surface, since the interactions between layers are only weak van der Waals, and a good model of a nanotube surface due to the similarity in bonding [6,8]. For the 50 atom slab the total energy was converged to meV with a Monkhorst-Pack [26]  $\mathbf{k}$ -point mesh of  $3 \times$

$3 \times 1$  ( $\Gamma$  included), and a distance between slab images of 18.3 Å. The adatom was initially positioned over an asymmetric position on the surface, and the whole system was allowed to relax fully. The diffusion paths were calculated in a static approximation using the nudged elastic band method [27,28].

The equilibrium position (Fig. 1) of the adatom was found to be in a bridgelike structure, between two surface carbon atoms. This geometry is similar to previous local density approximation (LDA) calculations [8,17,18] on a similar surface. The perpendicular distance of the adatom to the graphite surface is 1.87 Å. The adsorption energy of the defect was found by moving the adatom far from the surface until total energy convergence, and once again fully relaxing the surface to find the difference in energy. Note that the ground state for the isolated carbon atom is a triplet state, and we use this as a reference for our adsorption energies (to compare with adsorption energies referenced to the singlet state, 1.26 eV should be added to the values). The adsorption energy was found to be 1.40 eV (1.37 eV for the 72 atom slab). This is similar to the 1.2 eV [18] and 1.78 eV [8] found in finite cluster LDA studies, but smaller, even when comparing with the singlet reference adsorption energy of 2.66 eV, than the 3.30 eV found in previous periodic LDA works [17]. We also considered adsorption of an adatom directly on top of a surface carbon and found this to be over 1.0 eV higher in energy than the bridge structure.

In contrast to previous studies, we used fully spin-polarized DFT in our calculations and found that the ground state for the adsorbed adatom has a magnetic moment of  $0.45 \mu_B$ . Earlier finite cluster LDA calculations [18] also found a magnetic ground state for an adatom adsorbed on graphite, but they considered only a triplet solution, rather than the full unrestricted spin solution. If we restrict our system to zero spin ground state only ( $S = 0$ ), then the total energy is 35.5 meV higher than the magnetic configuration. Figure 2(a) shows clearly that the spin-polarized density occupies  $p$  orbitals of the adatom. The magnetic properties of the C adatom on graphene can be explained via a simple counting argument. Both the two bonded atoms on the surface, as well as the adatom, present a different hybridization: the surface atoms attached to the adatom have a  $sp^2$ - $sp^3$  hybridization while

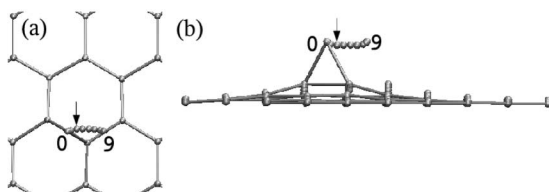


FIG. 1. The adatom equilibrium bridgelike position (0) and the diffusion path (0–9) from the (a) top and the (b) side. The arrows mark the magnetic transition point where the magnetic moment vanishes.

the adatom stays  $sp^2$  like, as seen in the model of Fig. 2(b). Concerning the adatom, the counting of the four carbon electrons is as follows: two electrons participate in the covalent bond with the graphene carbons. From the two remaining electrons, one goes to the dangling  $sp^2$  bond, and another is shared between the  $sp^2$  bond and the  $p_z$  orbital. This  $p_z$  orbital is orthogonal to the surface  $\pi$  orbitals due to symmetry and cannot form any bands, remaining localized and therefore spin polarized. The dangling  $sp^2$  bond will also probably be very slightly spin polarized, but this effect is negligibly small and cannot be seen in Fig. 2(a). Recent results on other surfaces [29–31] demonstrated that this behavior is typical for low-dimensional systems. The half electron of the  $p_z$  orbital provides the magnetization of around  $0.5 \mu_B$ . In addition the  $sp^2$ - $sp^3$  hybridization of the graphene carbon linked to the adatom decides the adsorption energetics of the adatom. Hence this counting discussion would be also relevant for the energetics in nanotubes, where the  $sp^2$ - $sp^3$  hybridization, although influenced by tube curvature, would again determine the adsorption energies [32].

We want to point out that the magnetic state is not dependent on the size of the cell, since it is consistently the ground state for the 50, 72, and 98 atom slabs. We can also consider how the difference between paramagnetic

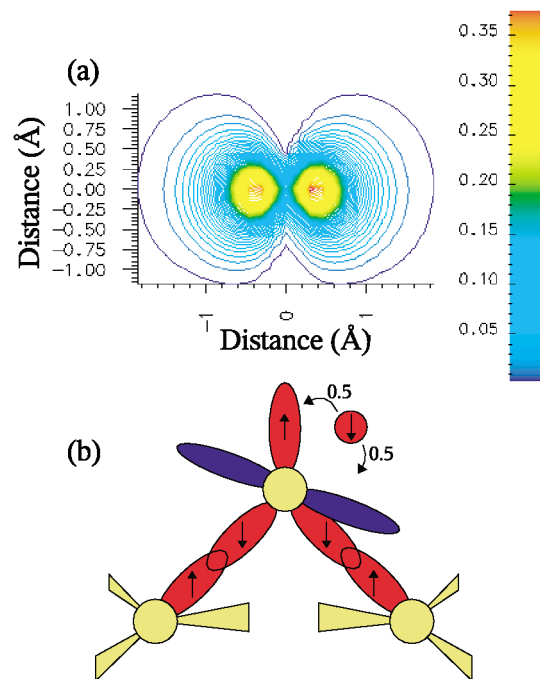


FIG. 2 (color). (a) The spin density in  $e/\text{Å}^3$  of a plane normal to the surface through the center of the adatom when the adatom is at the equilibrium position. The adatom is at (0,0). (b) A schematic diagram of the bond orbitals at the equilibrium position in a plane through the adatom and the two surface carbons. Note that this schematic is a projection, and that the blue  $p$  orbital is orthogonal to the adatom-surface bonds.

( $S = 0$ ) and ferromagnetic energies varies as a function of the cell size. When increasing the cell size, the difference oscillates, with a variation larger than the coupling in metallic multilayers [33], typically of the order of few meV. This oscillatory behavior points to a RKKY interaction [33] between the adatoms via the graphene surface. In the range of sizes where we are working (50–98 atoms), the zero coupling limit has not been reached yet, which indicates that the defects with a surface concentration of around 1% are still coupled. Although further calculations are needed in order to refine this issue, the ferromagnetic-paramagnetic energy difference can be ascribed to a Curie temperature of 100–200 K.

The adatom diffusion path is an almost straight line between equivalent sites bridging two surface carbon atoms. Figure 1 shows that the minimum energy path is slightly shifted into the interstitial space in the surface and also slightly nearer the surface than the equilibrium site. The spin-polarized diffusion barrier (see Fig. 3) is 0.47 eV. This result contrasts with Heggie *et al.* [18] who, using LDA and a finite cluster, predicted a diffusion path via an on-top site, with a barrier of only 0.1 eV. Note that the migration energy in bulk graphite may also contain contributions from other diffusion processes due to the presence of a “surface” on either side of the adatom. However, diffusion through the graphene layer, even via an interstitialcy mechanism, is predicted to have a barrier of over 4 times the value we predict for in-plane diffusion [3], hence migration along the graphene plane will dominate. During the diffusion the magnetic moment vanishes and this point is marked with an arrow in Fig. 1, and it occurs at position 3 in Fig. 3. The spin density at this point is 5 orders of magnitude smaller than for the equilibrium position—effectively zero. To check that the transition from magnetic to nonmagnetic configuration was not an artifact, we reran positions 3 and 4 directly with a large

initial magnetic “kick.” In both cases the nonmagnetic configuration remained the ground state.

When considering the transition state of the diffusion, the simple counting argument discussed previously must be modified. Electron counting would predict a magnetic moment of  $1\mu_B$ , while the calculations show no spin polarization. At the transition point the adatom has only one direct bond to the surface and the hybridization changes to  $sp$  like. This means there is now two free  $p$  orbitals into which the extra electron goes and they are also free to align with the surface  $\pi$  orbitals forming bands. The result is a much more delocalized density and the magnetism is destroyed. The ground state during diffusion is once again magnetic at position 7, as the adatom moves to an equivalent bridgelike adsorption site at position 9. The spin restricted diffusion barrier was only 0.43 eV, although the diffusion path remains very similar. In both cases we see that the predicted diffusion barriers are small, and, as expected from experiments [3], adatoms are highly mobile on the surface.

The physical consequences of the magnetic nature of this defect for the adsorption and diffusion processes are not huge—changes of only tenths of an eV between magnetic and nonmagnetic cases. However, the fact that this common intrinsic carbon defect is magnetic suggests that it is highly probable that it plays a role in the magnetism observed experimentally in several pure carbon systems [11,13,14]. In these experiments great care was taken to eliminate magnetic impurities from the system, yet residual magnetism was observed. Speculation was made that intrinsic carbon defects could be responsible, and here we have shown that a specific intrinsic carbon defect is magnetic.

The nature of these defects means that they are readily accessible to detection by magnetic experimental techniques such as electron spin resonance (ESR). The lines of the ESR spectra will originate from the nuclear spin in carbon, and further structure will appear as extra lines, probably around the first and above the last lines in the spectra. These  $^{13}\text{C}$  ESR satellite spectra may contain information about the adatom interaction with the graphene. In an effort to make some predictions with regard to possible signals generated by these defects we have applied the Karplus-Fraenkel relation [34,35]. We first integrated the spin density in spheres of increasing radii around the relevant atoms. In the adatom the magnetization increases until it saturates to the cell value. Around the nearest carbons to the adatom, the magnetization shows a negative minimum around  $0.7 \text{ \AA}$ , close to half the distance to the adatom, followed by a sharp increase due to contributions from the adatom. This minimum corresponds to a negative spin polarization with respect to the adatom, i.e., they are antiferromagnetically coupled, although the polarization values are very small. This follows the trends found in magnetic semiconductors [36]. From these values we can then estimate a rough

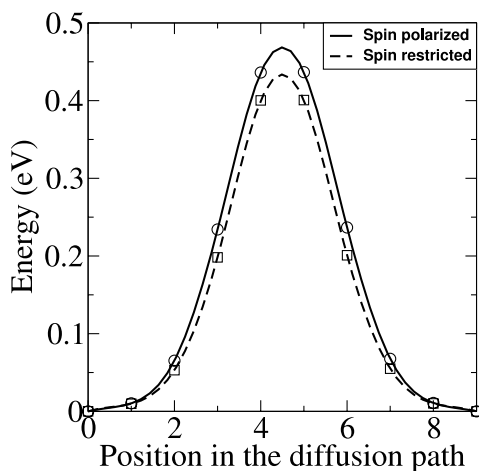


FIG. 3. Calculated energy barrier for diffusion of the adatom in the spin-polarized and the spin restricted case ( $S = 0$ ). The data points are fitted with a cubic spline.

picture for the hyperfine coupling constant. Using a  $sp^2$  interpretation, the calculated hyperfine coupling constants  $a_c$  are 2.32 and  $-2.02$  G for the adatom and its nearest neighbors, respectively. In addition, as the adatom and next neighbor atoms are in a ratio of 1:2, the signal change with the temperature will follow the same proportion.

The possibility of identifying and controlling the magnetic properties of carbon systems via careful preparation seems within grasp. The high mobility of the adatoms means that at high temperatures they should be more or less immediately annihilated by recombination, and their magnetic influence should be removed. Also, the calculations predict that the adatoms will diffuse as nonmagnetic species, only becoming magnetic at the equilibrium position. However, some clustering of adatoms is likely to occur, pinning the adatoms and producing some residual magnetism even at high temperatures. The exact magnetic nature of adatom clusters is not immediately clear, although it has been shown that Al adatoms retain their magnetism even for an infinite chain [30]. Further studies of the magnetic properties of larger defect clusters are in progress.

This work is supported by the Academy of Finland through its Centers of Excellence Program (2000–2005). We are grateful to the Center for Scientific Computing, Espoo, for use of its computational resources. The LEV00 code [37] was used for the calculation of density maps.

- 
- [1] R. Saito, M. Fujita, G. Dresselhaus, and M. S. Dresselhaus, *Physical Properties of Carbon Nanotubes* (Imperial College London Press, London, 1998).
- [2] P. M. Ajayan, *Chem. Rev.* **99**, 1787 (1999).
- [3] F. Banhart, *Rep. Prog. Phys.* **62**, 1181 (1999).
- [4] T. Maltezopoulos, A. Kubetzka, M. Morgenstern, and R. Wiesendanger, *Appl. Phys. Lett.* (to be published).
- [5] M. Bockrath, W. J. Liang, D. Bozovic, J. H. Hafner, C. M. Lieber, M. Tinkham, and H. Park, *Science* **291**, 283 (2001).
- [6] G. G. Samsonidze, G. G. Samsonidze, and B. I. Yakobson, *Phys. Rev. Lett.* **88**, 065501 (2002).
- [7] V. Meunier, J. Kephart, C. Roland, and J. Bernholc, *Phys. Rev. Lett.* **88**, 075506 (2002).
- [8] Y. H. Lee, S. G. Kim, and D. Tománek, *Phys. Rev. Lett.* **78**, 2393 (1997).
- [9] M. Ouyang, J. L. Huang, C. L. Cheung, and C. M. Lieber, *Science* **291**, 97 (2001).
- [10] M. T. Woodside and P. L. McEuen, *Science* **296**, 1098 (2002).
- [11] T. L. Makarova, B. Sundqvist, R. Höhne, P. Esquinazi, Y. Kopelevich, P. Scharff, V. A. Davydov, L. S. Kashevarova, and A. V. Rakhmanina, *Nature (London)* **413**, 716 (2001).
- [12] S. Bandow, F. Kokai, K. Takahashi, M. Yudasaka, and S. Iijima, *Appl. Phys. A* **73**, 281 (2001).
- [13] P. Esquinazi, A. Setzer, R. Höhne, C. Semmelhack, Y. Kopelevich, D. Spemann, T. Butz, B. Kohlstrunk, and M. Lösche, *Phys. Rev. B* **66**, 024429 (2002).
- [14] R. A. Wood, M. H. Lewis, M. R. Lees, S. M. Bennington, M. G. Cain, and N. Kitamura, *J. Phys. Condens. Matter* **14**, L385 (2002).
- [15] J. M. D. Coey, M. Venkatesan, C. B. Fitzgerald, A. P. Douvalis, and I. S. Sanders, *Nature (London)* **420**, 156 (2002).
- [16] M. Freitag, A. T. Johnson, S. V. Kalinin, and D. A. Bonnell, *Phys. Rev. Lett.* **89**, 216801 (2002).
- [17] K. Nordlund, J. Keinonen, and T. Mattila, *Phys. Rev. Lett.* **77**, 699 (1996).
- [18] M. Heggie, B. R. Eggen, C. P. Ewels, P. Leary, S. Ali, G. Jungnickel, R. Jones, and P. R. Briddon, *Electrochem. Soc. Proc.* **6**, 60 (1998).
- [19] B. Hammer, K. W. Jacobsen, and J. K. Nørskov, *Phys. Rev. Lett.* **70**, 3971 (1993).
- [20] J. A. White, D. M. Bird, M. C. Payne, and I. Stich, *Phys. Rev. Lett.* **73**, 1404 (1994).
- [21] G. Kresse and J. Furthmüller, *Comput. Mater. Sci.* **6**, 15 (1996).
- [22] G. Kresse and J. Furthmüller, *Phys. Rev. B* **54**, 11169 (1996).
- [23] J. P. Perdew, J. A. Chevary, S. H. Vosko, K. A. Jackson, M. R. Pederson, D. J. Singh, and C. Fiolhais, *Phys. Rev. B* **46**, 6671 (1992).
- [24] G. Kresse and J. Joubert, *Phys. Rev. B* **59**, 1758 (1999).
- [25] P. E. Blöchl, *Phys. Rev. B* **50**, 17953 (1994).
- [26] H. J. Monkhorst and J. D. Pack, *Phys. Rev. B* **13**, 5188 (1976).
- [27] G. Mills, H. Jonsson, and G. K. Schenter, *Surf. Sci.* **324**, 305 (1995).
- [28] *Classical and Quantum Dynamics in Condensed Phase Simulations*, edited by B. J. Berne, G. Ciccotti, and D. F. Coker (World Scientific, London, 1998).
- [29] S. Watanabe, M. Ichimura, T. Onogi, Y. A. Ono, T. Hashizume, and Y. Wada, *Jpn. J. Appl. Phys.* **36**, L929 (1997).
- [30] A. Ayuela, H. Raebiger, M. J. Puska, and R. M. Nieminen, *Phys. Rev. B* **66**, 035417 (2002).
- [31] N. Zabala, M. J. Puska, H. Raebiger, and R. M. Nieminen, *J. Magn. Magn. Mater.* **249**, 193 (2002).
- [32] A. Krasheninnikov, K. Nordlund, P. O. Lehtinen, A. S. Foster, A. Ayuela, and R. M. Nieminen (to be published).
- [33] P. Bruno and C. Chappert, *Phys. Rev. B* **46**, 261 (1992).
- [34] G. Seifert, A. Bartl, L. Dunsch, A. Ayuela, and A. Rockenbauer, *Appl. Phys. A* **66**, 265 (1998).
- [35] M. Karplus and G. K. Fraenkel, *J. Chem. Phys.* **35**, 1312 (1961).
- [36] S. Sanvito, P. Ordejón, and N. A. Hill, *Phys. Rev. B* **63**, 165206 (2001).
- [37] L. N. Kantorovich, [www.cmp.ucl.ac.uk/~lev](http://www.cmp.ucl.ac.uk/~lev)